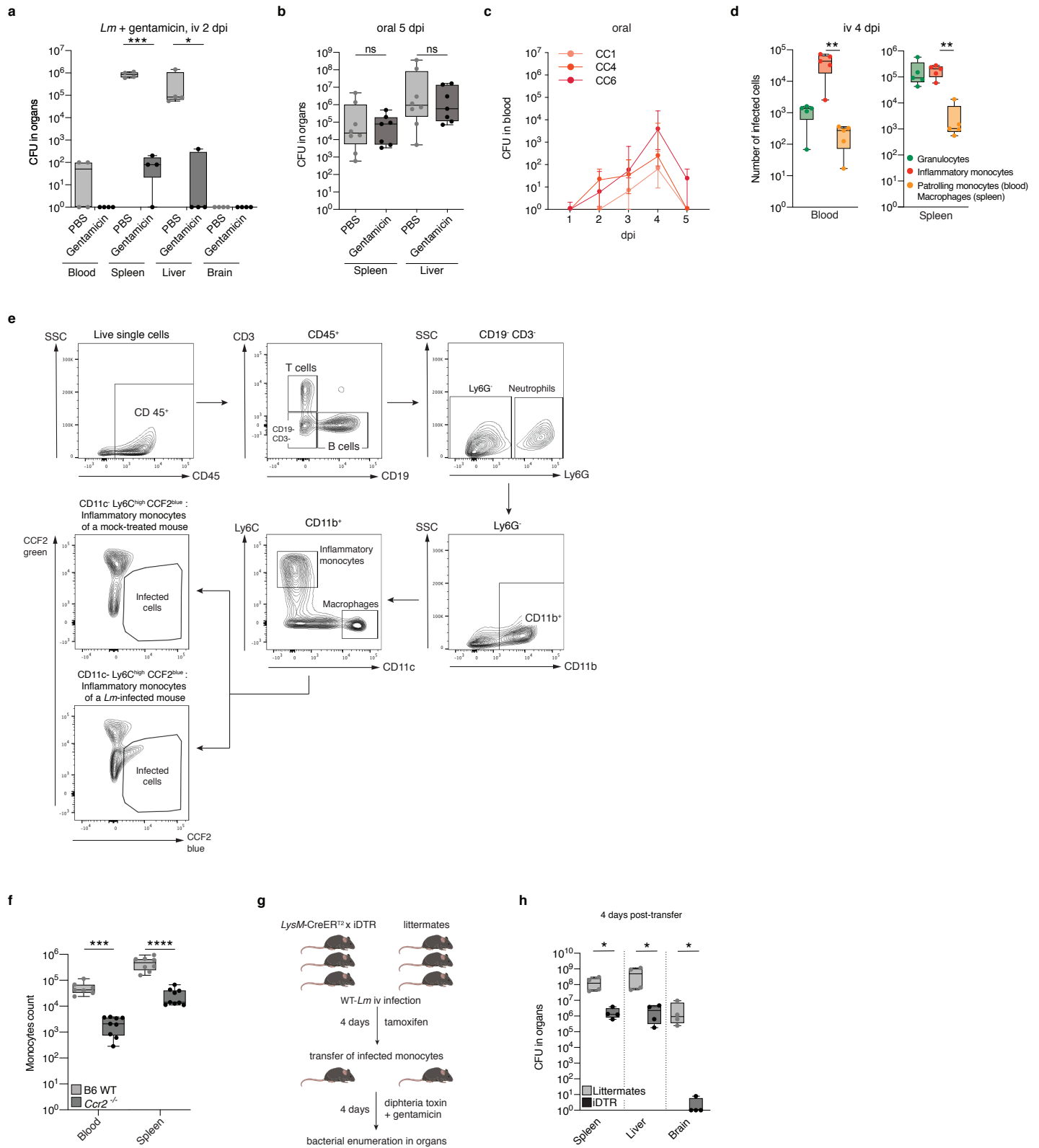
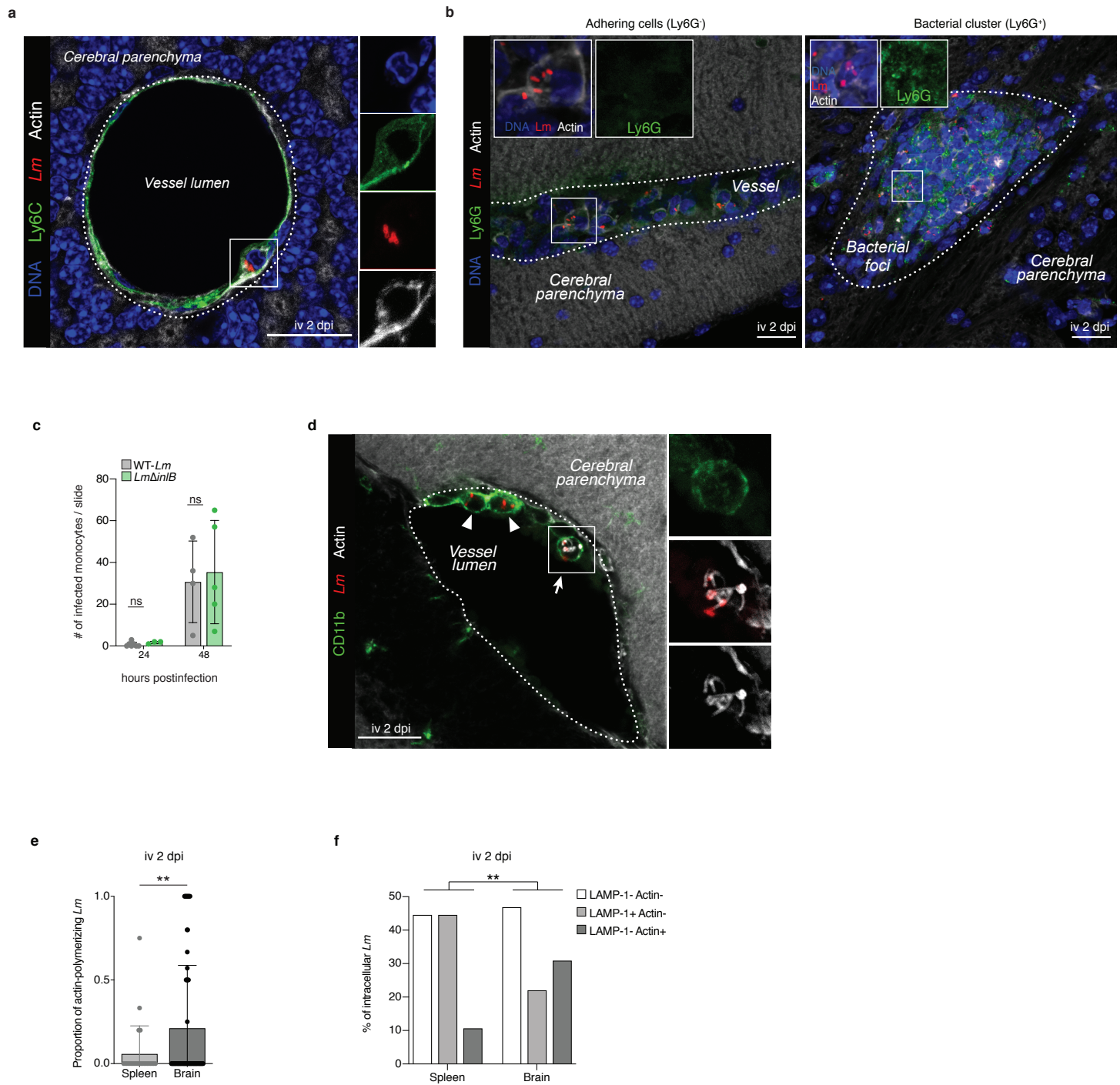


# Extended Data Figure 1



1 **Extended Data Fig. 1. Infected inflammatory monocytes are necessary for *Lm* to invade the**  
2 **CNS. (a)** Bacterial load in organs of KIE16P mice 2 days after iv inoculation with  $10^4$  CFU CC4-  
3 *Lm* immediately followed by injection of gentamicin, assessing the bactericidal effect of  
4 gentamicin on extracellular circulating *Lm*. **(b)** Bacterial load in the spleen and liver 5 days after  
5 oral inoculation with  $2 \times 10^8$  CFU CC4-*Lm*, in KIE16P mice treated with gentamicin every day  
6 from day 1 post-inoculation, related to Fig. 1A. **(c)** Bacterial load in the blood of KIE16P mice  
7 after oral inoculation with  $2 \times 10^8$  CFU of CC1/CC4/CC6-*Lm*, related to Fig. 1A. **(d)** Repartition of  
8 the 3 main infected cell subsets in the blood and spleen of KIE16P mice 4 days after iv inoculation  
9 with  $10^4$  CFU of CC4-*Lm*. **(e)** Representative dot plots of the gating strategy used for flow  
10 cytometry analysis. Infected cells are identified through the shift of fluorescence, upon excitation  
11 with the 405 nm laser, of the CCF2-AM substrate from green (518 nm) to blue (447 nm) in  
12 presence of  $\beta$ -lactamase expressing-*Lm*. **(f)** Number of inflammatory monocytes in the blood and  
13 spleen of B6-WT or *Ccr2*<sup>-/-</sup> mice. **(g)** Schematic pipeline of the transfer experiment in *LysM*-  
14 *CreER*<sup>T2</sup>  $\times$  iDTR mice. **(h)** Bacterial load in the spleen, liver and brain of gentamicin- and  
15 diphtheria toxin-treated recipient *LysM-CreER*<sup>T2+/-</sup>  $\times$  *Rosa26-iDTR*<sup>+/+</sup> and littermates mice, 4 days  
16 after injection of infected monocytes harvested from  $n = 3$  donor tamoxifen-treated *LysM*-  
17 *CreER*<sup>T2+/-</sup>  $\times$  *Rosa26-iDTR*<sup>+/+</sup> or  $n = 3$  littermates mice, 4 days after iv inoculation with  $10^4$  CC4-  
18 WT. Data were obtained from two (a) or three (b-d, f) and four (h) independent experiments and  
19 are presented as median  $\pm$  interquartile (box) and extreme values (lines) (a-b, d, f and h) or as  
20 median  $\pm$  interquartile (c). Samples are compared with an unpaired Mann-Whitney test (a-b, f and  
21 h) and number of infected cells with the Friedman test (d). ns:  $p > 0.05$ , \*:  $p < 0.05$ , \*\*:  $p < 0.01$ , \*\*\*:  
22  $p < 0.001$ , \*\*\*\*:  $p < 0.0001$ .

## Extended Data Figure 2



24 **Extended Data Fig. 2. Infected inflammatory monocytes transfer *Lm* to the CNS. (a-b)**

25 Representative fluorescence microscopy images of infected inflammatory monocytes adhering to  
26 endothelial cells 2 days after iv inoculation with  $5 \times 10^5$  CFU CC1-*Lm* in KIE16P mice. Adhering  
27 infected cells are Ly6C<sup>+</sup> (a) and Ly6G<sup>-</sup> (b left panel; to ensure the specificity of the Ly6G<sup>-</sup> staining  
28 we show in the right panel a positive control staining for Ly6G in a parenchymal bacterial cluster).

29 **(c)** Quantification of infected monocytes in brain vessels of KIE16P mice 24 and 48 hours after iv  
30 inoculation with  $5 \times 10^5$  CFU CC4-*Lm* and CC4 $\Delta$ inlB. Each dot corresponds to the average number

31 of monocytes counted on two slides (representative median sagittal sections, 40  $\mu$ m thickness) for

32 one mouse. **(d)** Representative fluorescence microscopy images of infected inflammatory  
33 monocytes adhering to endothelial cells 2 days after iv inoculation of  $5 \times 10^5$  CFU CC1-*Lm* in

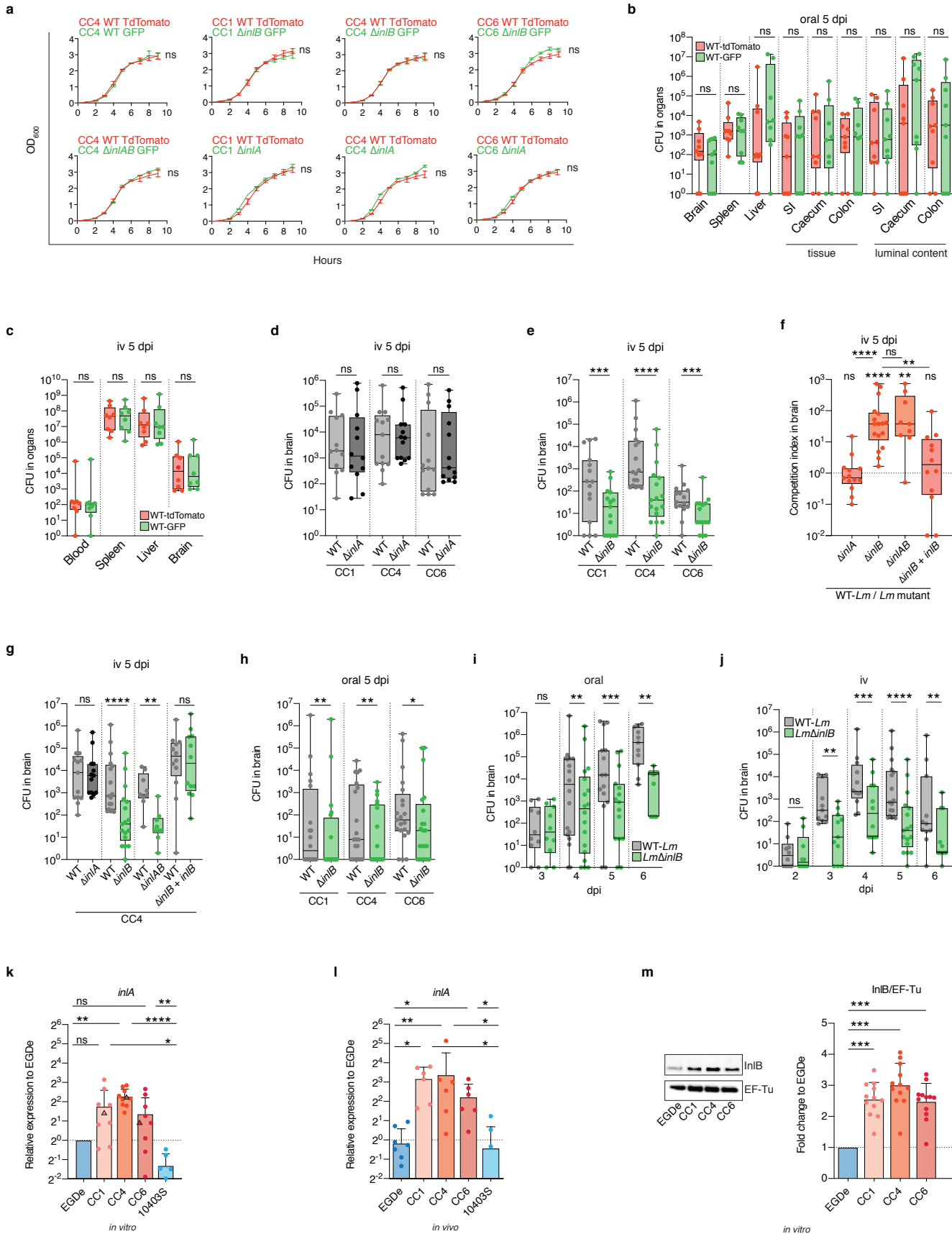
34 KIE16P mice, in which intra-monocytic *Lm* are found polymerizing host actin. **(e, f)** Proportion of

35 actin-polymerizing *Lm* (e) and *Lm* co-localizing with either LAMP-1 or Actin (f) in spleen and  
36 brain of KIE16P mice 3 days after iv inoculation with  $10^4$  CC4-*Lm*. Scale bars: 20  $\mu$ m, **a** and **d** are

37 maximum intensity projections over a *z*-stack. Data were obtained from three independent

38 experiments and are presented as mean  $\pm$  SD. Samples are compared with an unpaired Mann-  
39 Whitney test (c and e) and a one-way ANOVA (f). ns:  $p > 0.05$ , \*\*:  $p < 0.01$ .

# Extended Data Figure 3



41 **Extended Data Fig. 3. InlB is a major determinant of *Lm* neuroinvasiveness whereas InlA is**  
42 **not.** (a) Optical density of indicated bacterial strains measured every hour for 9 hours after 1:100  
43 dilution in BHI of an overnight culture. (b and c) Bacterial load in organs or luminal contents of  
44 KIE16P mice 5 days after oral inoculation with  $2 \times 10^8$  CFU (b) or after iv inoculation with  $10^4$   
45 CFU (c) of 1:1 CC4-WT expressing TdTomato or GFP. (d) Bacterial load in brain of KIE16P mice  
46 5 days after iv inoculation with  $10^4$  CFU of 1:1 mix of WT and  $\Delta inlA$  isogenic strains, related to  
47 Fig. 2a. (e) Bacterial load in brain of KIE16P mice 5 days after iv inoculation with  $10^4$  CFU of 1:1  
48 mix of WT and  $\Delta inlB$  isogenic strains, related to Fig. 2b. (f, g) Competition index (f) and bacterial  
49 load (g) in brain of KIE16P mice 5 days after iv inoculation with  $10^4$  CFU of 1:1 mix of CC4-WT  
50 and either CC4 $\Delta inlA$ , CC4 $\Delta inlB$ , CC4 $\Delta inlAB$  or CC4 $\Delta inlB$  complemented with *inlB*, related to  
51 Fig. 2a-b and panels d,e. (h) Bacterial load in brain of KIE16P mice 5 days after oral inoculation  
52 with  $2 \times 10^8$  CFU of 1:1 mix of WT strain and  $\Delta inlB$  isogenic strains, related to Fig. 2c. (i, j)  
53 Bacterial load in brain of KIE16P mice at indicated times after oral inoculation with  $2 \times 10^8$  CFU  
54 (i) and after iv inoculation with  $10^4$  CFU (j) of 1:1 CC4-WT and CC4 $\Delta inlB$ , related to Fig. 2f, g.  
55 (k) Transcription levels of *inlA* relative to EGDe in mid-log phase in BHI. For CC1/4/6, each dot  
56 corresponds to a different clinical isolate and triangles represent the strains used throughout the  
57 rest of the study and referred to as CC1, CC4 and CC6, related to Fig. 2h. (l) Transcription levels  
58 of *inlA* relative to EGDe in infected splenocytes 2 days after iv inoculation with  $2 \times 10^5$  CFU in  
59 KIE16P mice, related to Fig. 2i. (m) Representative Western blot (left) and quantification (right)  
60 of InlB expression, normalized to that of EF-Tu, relative to EGDe in mid-log phase in BHI. Data  
61 were obtained from three (a-l) and four (m) independent experiments and are presented as mean  $\pm$   
62 SD (a, k-m) or as median  $\pm$  interquartile (box) and extreme values (lines) (b-j). Curves were fitted  
63 with a Gompertz model and the lag phases (k) for each pair of *Lm* strains were compared with the

64 extra sum-of-squares F test (a). CFU in competition assays are compared with the Wilcoxon  
65 matched-pairs signed rank test (b-j) and samples compared with the Kruskal-Wallis test (f, k-m).

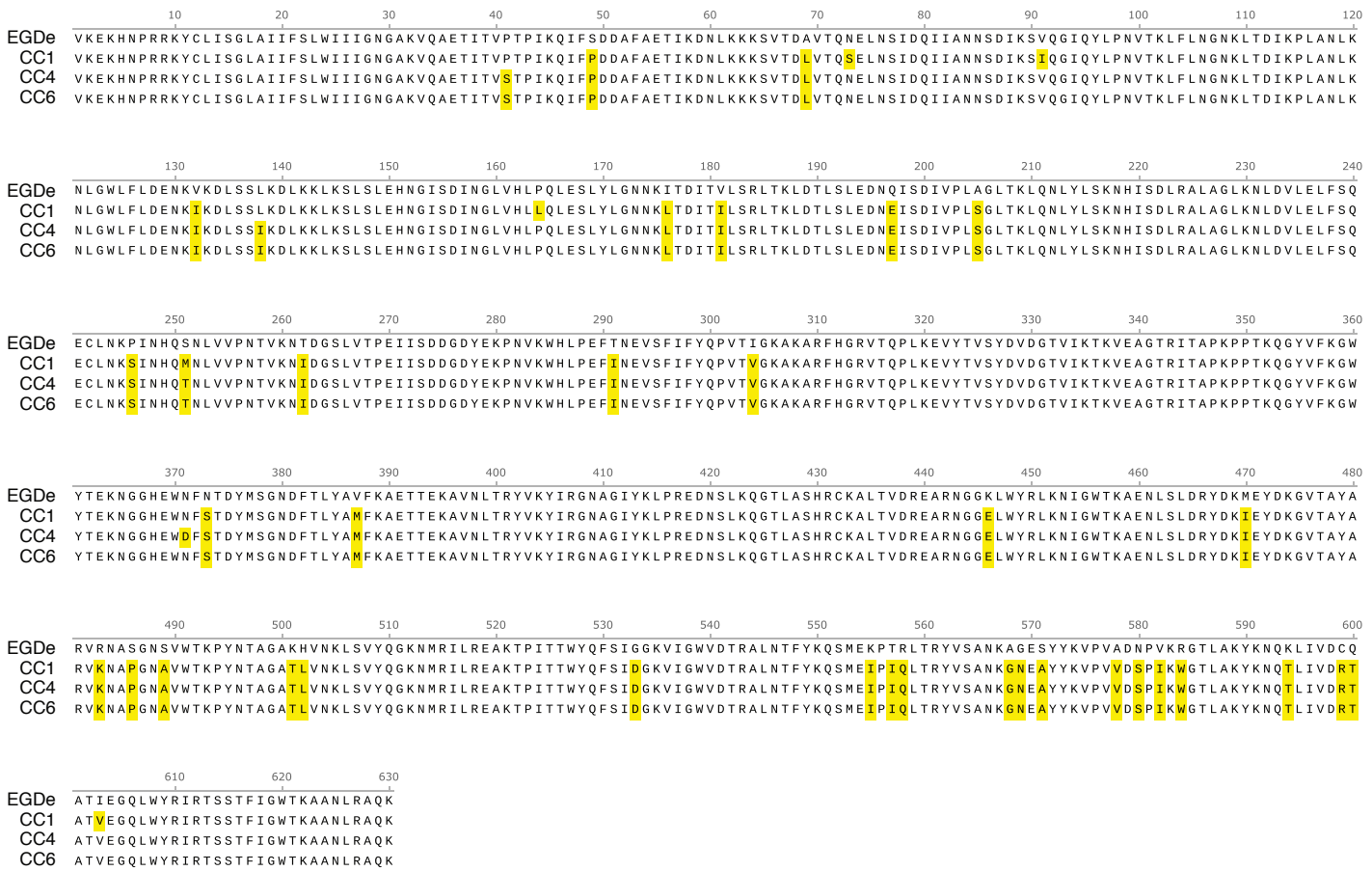
66 ns:  $p>0.05$ , \*:  $p<0.05$ , \*\*:  $p<0.01$ , \*\*\*:  $p<0.001$ , \*\*\*\*:  $p<0.0001$ .

67

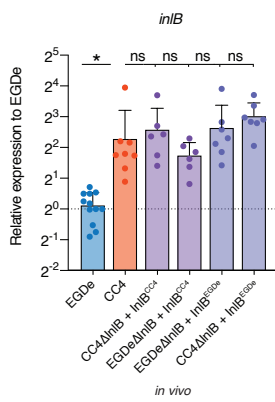
# Extended Data Figure 4

a

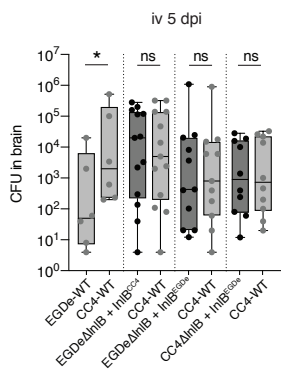
InlB sequence



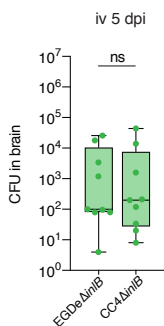
b



c

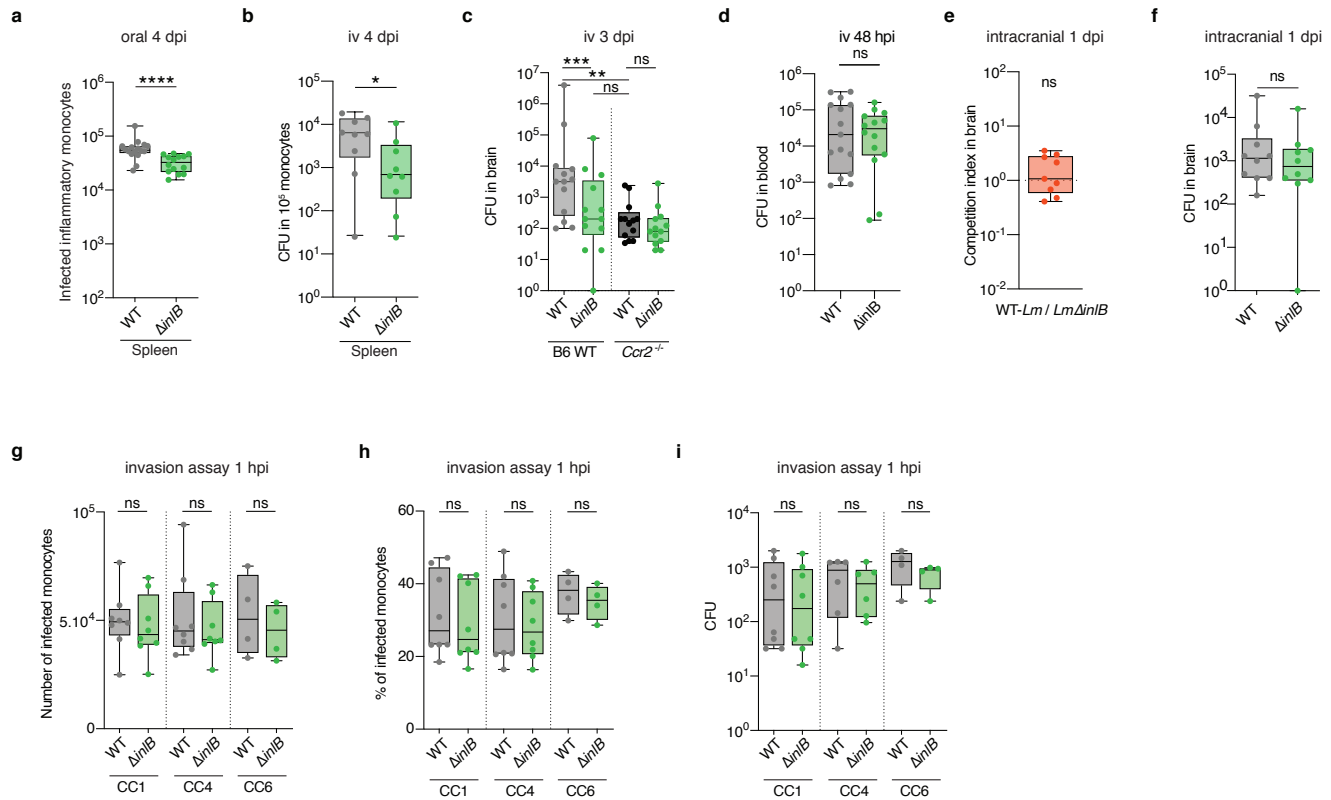


d



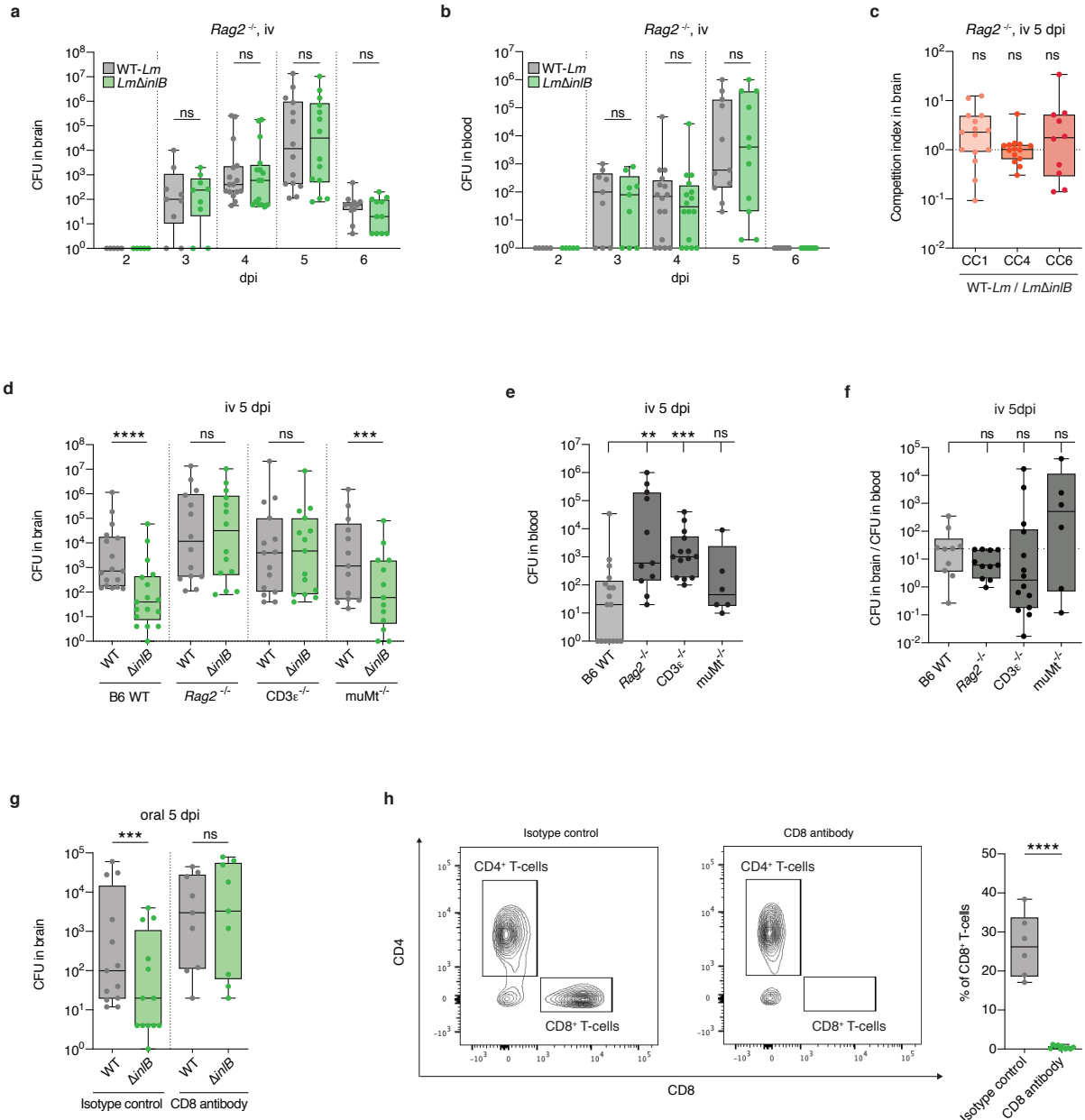
68 **Extended Data Fig. 4. Levels of expression of InlB, and not allelic differences with EGDe,**  
69 **explain enhanced neuroinvasiveness of hypervirulent CC1, CC4 and CC6 strains. (a)** Protein  
70 sequence alignment of InlB alleles from EGDe and from CC1, CC4 and CC6 strains. Mismatches  
71 are indicated in yellow. **(b)** Transcription levels of *inlB*, relative to EGDe, in infected splenocytes  
72 2 days after iv inoculation with  $2 \times 10^5$  CFU in KIE16P mice of EGDe-WT, CC4-WT and strains  
73 complemented with either InlB from EGDe or from CC4. **(c)** Bacterial load in brain of KIE16P  
74 mice 5 days after iv inoculation with  $10^4$  CFU of a 1:1 mix of the indicated bacterial strains, related  
75 to Fig. 2j. **(d)** Bacterial load in brain of KIE16P mice 5 days after iv inoculation with  $2 \times 10^4$  CFU  
76 of a 1:1 mix of EGDe $\Delta$ *inlB* and CC4 $\Delta$ *inlB*, related to Fig. 2j. Data were obtained from three  
77 independent experiments and are presented as mean  $\pm$  SD (b) or as median  $\pm$  interquartile (box)  
78 and extreme values (lines) (c-d). CFU in competition assays are compared with the Wilcoxon  
79 matched-pairs signed rank test (c-d) and samples compared with the Kruskal-Wallis test (b). ns:  
80  $p > 0.05$ , \*:  $p < 0.05$ .

## Extended Data Figure 5



82 **Extended Data Fig. 5. InlB is not involved in *Lm* invasion in monocytes.** (a) Number of infected  
83 monocytes in the spleen of KIE16P mice 4 days after oral inoculation with  $2 \times 10^8$  CFU of CC4-  
84 WT or CC4 $\Delta$ inlB. (b) Bacterial enumeration from sorted monocytes retrieved from KIE16P mice  
85 iv infected for 4 days with  $10^4$  CFU of CC4-WT or CC4 $\Delta$ inlB. (c) Bacterial load in brain of control  
86 or *Ccr2*<sup>-/-</sup> mice 3 days after iv inoculation with  $10^4$  CFU of 1:1 CC4-WT and CC4 $\Delta$ inlB. (d)  
87 Bacterial load in the brain 48 hours after iv inoculation of KIE16P mice with  $5 \times 10^5$  CFU of either  
88 CC4-WT strain or CC4 $\Delta$ inlB. (e, f) Competition index (e) and bacterial load (f) in the brain of  
89 KIE16P mice 1 day after intracranial inoculation with  $10^2$  CFU of 1:1 mix of CC4-WT and  
90 CC4 $\Delta$ inlB. (g-i) Number of infected monocytes (g), percentage of infected monocytes (h) and  
91 bacterial load (i) in monocytes 1 hour after *in vitro* infection of primary bone marrow mouse  
92 monocytes with WT-*Lm* or  $\Delta$ inlB isogenic mutant, at a MOI of 5. Data were obtained from three  
93 (d-f) and four (a-c, g-i) independent experiments and are presented as median  $\pm$  interquartile (box)  
94 and extreme values (lines). Samples are compared with the unpaired Mann-Whitney test (a-b, d,  
95 g-i) and the Kruskal-Wallis test (c), and CFU in competition assays are compared with the  
96 Wilcoxon matched-pairs signed rank test (c, e-f). ns:  $p > 0.05$ .

## Extended Data Figure 6

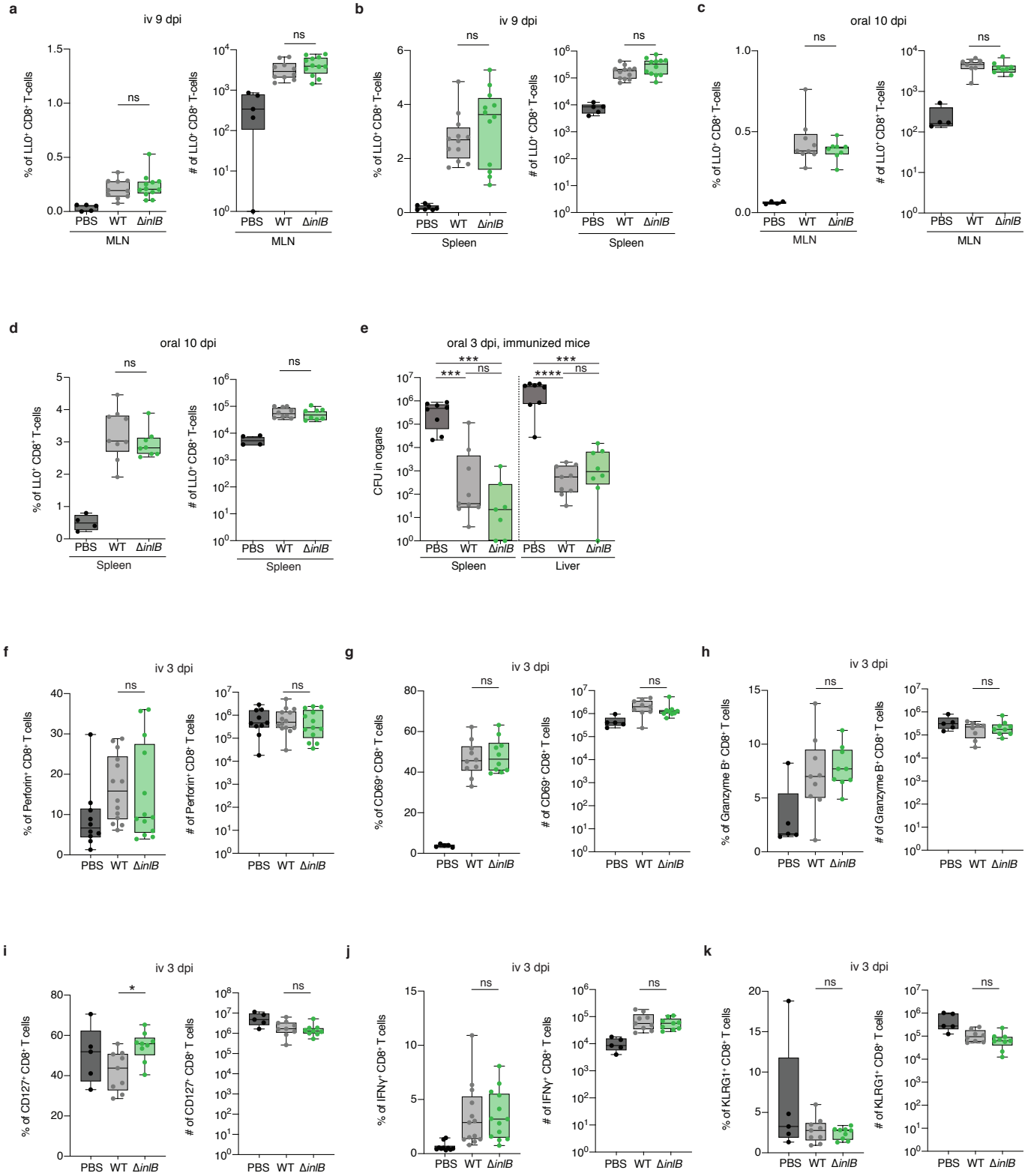


98 **Extended Data Figure 6. InlB-mediated *Lm* neuroinvasiveness is abrogated in CD8<sup>+</sup> T-cells**

99 **deficient mice.** (a, b) Bacterial load in brain (a) and in blood (b) of *Rag2*<sup>-/-</sup> mice after iv inoculation  
100 with 10<sup>4</sup> CFU of a 1:1 mix of CC4-WT and CC4 $\Delta$ *inlB*, related to Fig.3f (c) Competition index in  
101 brain of *Rag2*<sup>-/-</sup> mice 5 days after iv inoculation with 10<sup>4</sup> CFU of a 1:1 mix WT strain and  $\Delta$ *inlB*  
102 isogenic strains. (d, e) Bacterial load in brain (d) and in blood (e) 5 days after iv inoculation with  
103 10<sup>4</sup> CFU of 1:1 CC4-WT strain and CC4 $\Delta$ *inlB* isogenic mutant in control mice and in mice lacking  
104 functional T (CD3 $\varepsilon$ <sup>-/-</sup>), B lymphocytes (muMt<sup>-/-</sup>) or both (*Rag2*<sup>-/-</sup>), related to Fig. 3g. (f) Ratio of  
105 brain/blood bacterial load in control, *Rag2*<sup>-/-</sup>, CD3 $\varepsilon$ <sup>-/-</sup> and muMt<sup>-/-</sup> mice, related to Fig. 3g. (g)  
106 Bacterial load in brain of KIE16P mice 5 days after oral inoculation with 2 $\times$ 10<sup>8</sup> CFU of 1:1 CC4-  
107 WT and CC4 $\Delta$ *inlB* after CD8<sup>+</sup> T-cells depletion, related to Fig. 3h. (h) Representative dot plots  
108 (left) and proportion of CD8<sup>+</sup> T-cells (right) among CD45<sup>+</sup> CD3<sup>+</sup> cells in the spleen, after CD8<sup>+</sup>  
109 T-cells depletion, related to Fig. 3h. Data were obtained from three independent experiments and  
110 are presented as median  $\pm$  interquartile (box) and extreme values (lines). CFU in competition  
111 assays are compared with the Wilcoxon matched-pairs signed rank test (a-d and g) and samples  
112 are compared with the Kruskal-Wallis test (e, f) and with the Mann-Whitney test (h). ns:  $p>0.05$ ,  
113 \*\*:  $p<0.01$ , \*\*\*:  $p<0.001$ , \*\*\*\*:  $p<0.0001$ .

114

# Extended Data Figure 7

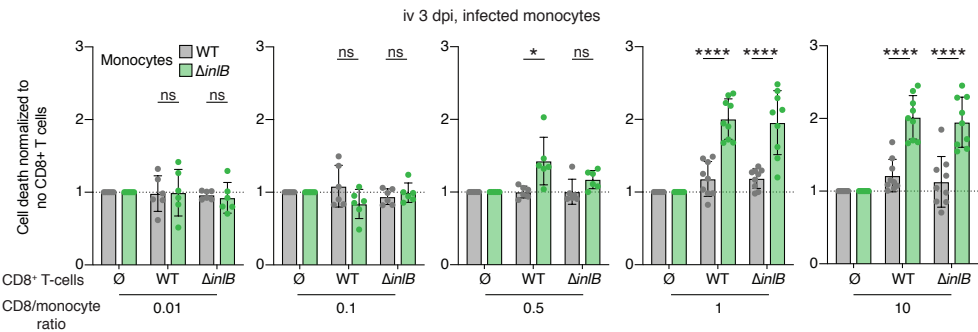


115 **Extended Data Figure 7. InlB does not alter the induction and differentiation of specific anti-**  
116 **Lm CD8<sup>+</sup> T-cells.** (a, b) Percentage (left) and number (right) of LLO-specific CD8<sup>+</sup> T-cells in  
117 mesenteric lymph nodes (MLN) (a) and spleen (b) of BALB/c mice 9 days after iv inoculation  
118 with  $1 \times 10^3$  of CC4-WT strain or CC4 $\Delta$ inlB. (c, d) Percentage (left) and number (right) of LLO-  
119 specific CD8<sup>+</sup> T-cells in mesenteric lymph nodes (MLN) (c) and spleen (d) of iFABP-hEcad mice  
120 10 days after oral inoculation with  $2 \times 10^7$  of CC4-WT strain or CC4 $\Delta$ inlB. (e) Bacterial load in  
121 spleen and liver 3 days after oral inoculation with  $1 \times 10^9$  CFU of CC4-WT in KIE16P mice  
122 challenged 30 days before with  $5 \times 10^7$  CFU of CC4-WT strain or CC4 $\Delta$ inlB. (f-k) Percentage (left)  
123 and number (right) of Perforin<sup>+</sup> (f), CD69<sup>+</sup> (g), Granzyme-B<sup>+</sup> (h), CD127<sup>+</sup> (i), IFN $\gamma$ <sup>+</sup> (j) and  
124 KLRG1<sup>+</sup> (k) CD8<sup>+</sup> T-cells 3 days after iv inoculation of KIE16P mice with  $10^4$  CFU of CC4-WT  
125 or CC4 $\Delta$ inlB. Data were obtained from three independent experiments and are presented as median  
126  $\pm$  interquartile (box) and extreme values (lines). Samples are compared with the Mann-Whitney  
127 test. ns:  $p > 0.05$ , \*\*\*:  $p < 0.001$ , \*\*\*\*:  $p < 0.0001$ .

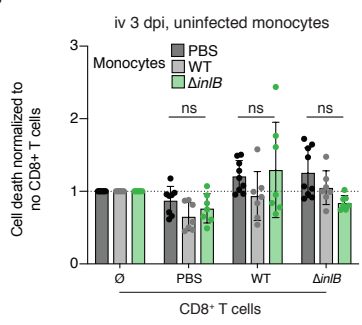
128

# Extended Data Figure 8

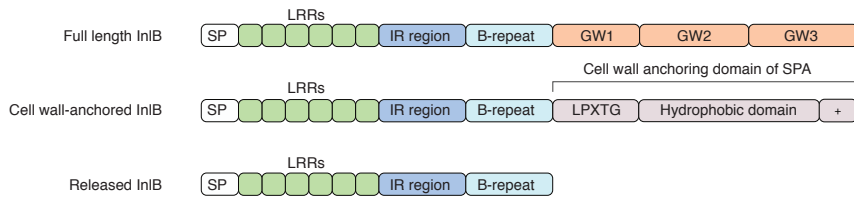
a



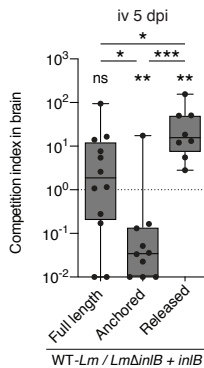
b



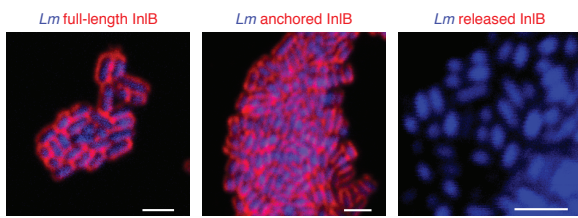
c



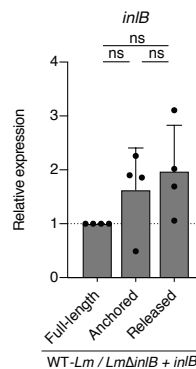
d



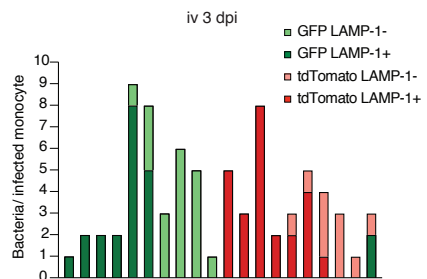
e



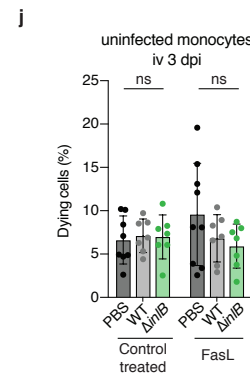
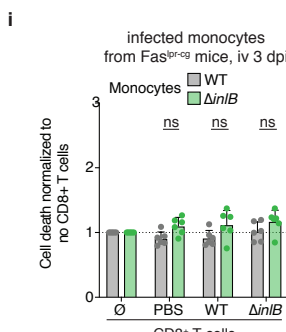
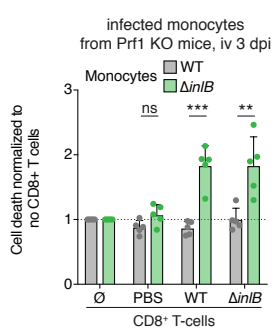
f



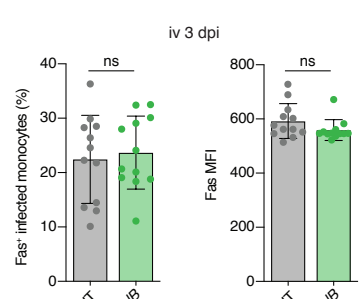
g



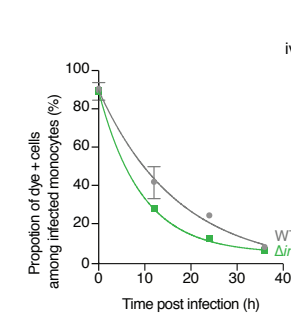
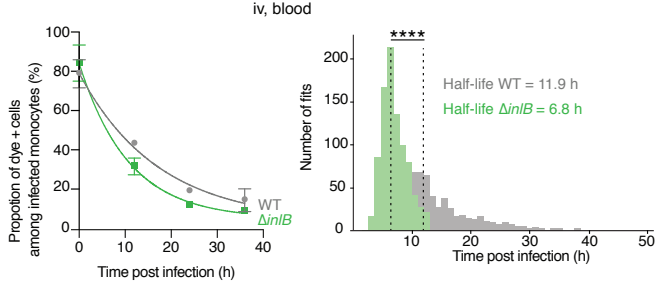
h



k



l



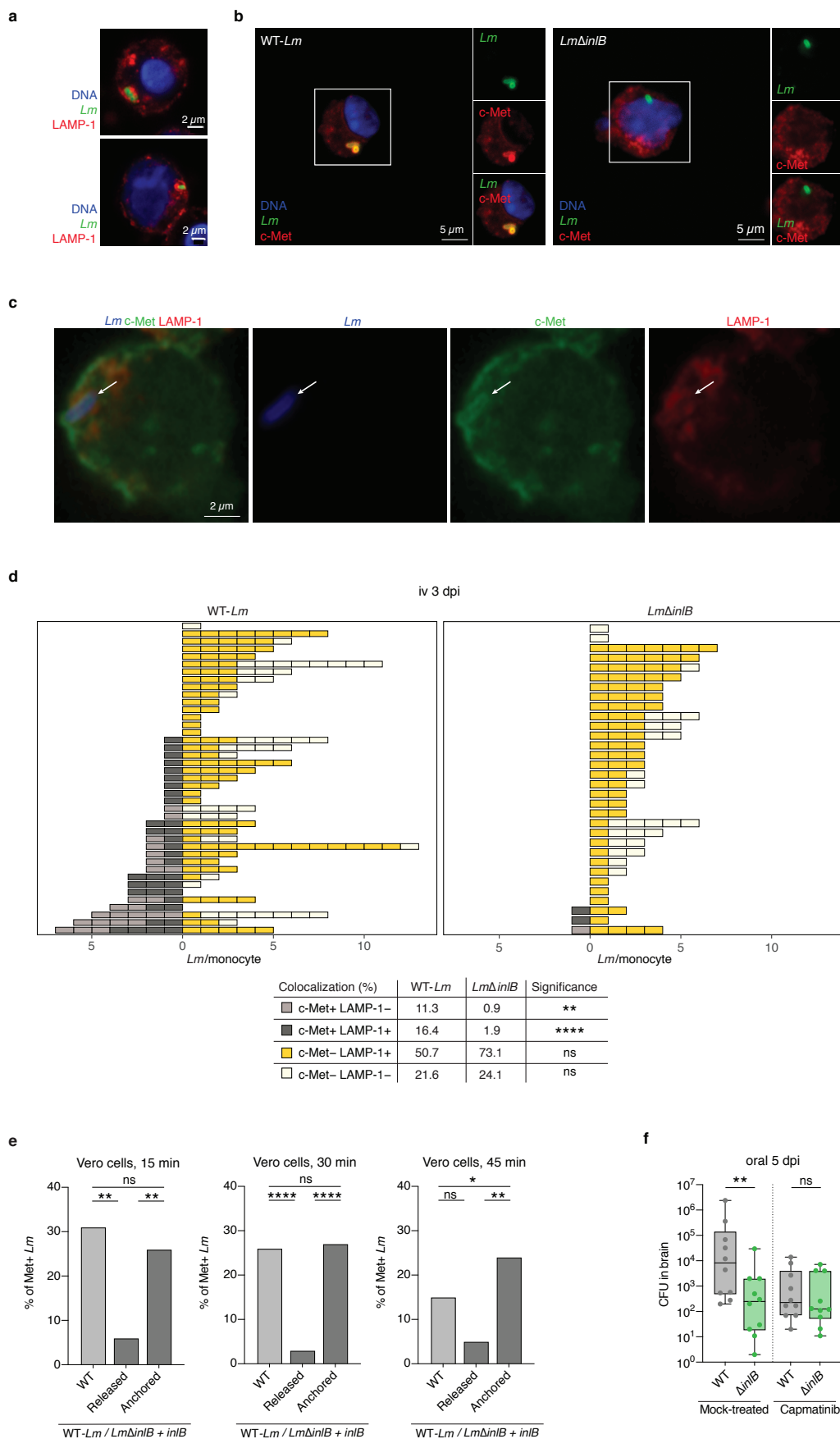
129 **Extended Data Figure 8. Membrane-associated InlB protects infected monocytes from CD8<sup>+</sup>**

130 **T cells-mediated cell death.** (a) Level of caspase-3 cleavage of infected spleen monocytes,  
131 harvested 3 days after iv infection with 10<sup>4</sup> CFU of CC4-WT or CC4 $\Delta$ inlB of KIE16P mice, and  
132 incubated with CD8<sup>+</sup> T-cells from similarly infected (WT and  $\Delta$ inlB) or control (PBS) mice at the  
133 indicated effector to target ratio, related to Fig. 3j. Results are normalized to the level of caspase-  
134 3 cleavage in absence of CD8<sup>+</sup> T cells. (b) Level of caspase-3 cleavage of uninfected spleen  
135 monocytes, harvested 3 days after iv infection with 10<sup>4</sup> CFU of CC4-WT or CC4 $\Delta$ inlB of KIE16P  
136 mice, and incubated with CD8<sup>+</sup> T-cells from similarly infected (WT and  $\Delta$ inlB) or control (PBS)  
137 mice at an effector to target ratio of 5, related to Fig. 3j. Results are normalized to the level of  
138 caspase-3 cleavage in absence of CD8<sup>+</sup> T cells. (c) Schematic representation of WT InlB and its  
139 anchored and released variants. (d) Competition index in the brain of KIE16P mice 5 days after iv  
140 inoculation with 10<sup>4</sup> CFU of 1:1 CC4-WT and CC4 $\Delta$ inlB transformed with a plasmid expressing  
141 either full-length WT InlB, cell wall-anchored InlB or released InlB. (e) Representative  
142 fluorescence microscopy images of centrifugated CC4 $\Delta$ inlB transformed with a plasmid  
143 expressing either full length InlB (left panel), anchored InlB (central panel) or released InlB (right  
144 panel). Scale bars: 5  $\mu$ m. (f) Transcription level of inlB in CC4 $\Delta$ inlB transformed with a plasmid  
145 expressing InlB variants in mid-log phase in BHI, relative to CC4 $\Delta$ inlB expressing full length InlB.  
146 (g) Proportion of GFP- or tdTomato-expressing bacteria, co-localizing or not with LAMP-1, in 20  
147 infected monocytes harvested 3 days after iv inoculation of KIE16P mice with 10<sup>4</sup> CFU of 1:1 mix  
148 of CC4-WT expressing GFP or tdTomato. (h, i) Level of caspase-3 cleavage of infected spleen  
149 monocytes, harvested from *Prf1* KO (h) or *Fas*<sup>lpr-cg</sup> (i) mice, 3 days after iv inoculation with 10<sup>4</sup>  
150 CFU of CC4-WT or CC4 $\Delta$ inlB, incubated with CD8<sup>+</sup> T-cells from similarly infected (WT and  
151  $\Delta$ inlB) or control (PBS) mice, at an effector to target ratio of 5. (j) Level of caspase-3 cleavage of

152 non-infected spleen monocytes, harvested from KIE16P mice iv infected for 3 days with  $10^4$  CFU  
153 of CC4-WT or CC4 $\Delta$ inlB, incubated *ex vivo* with Fas ligand, related to Fig. 3k. **(k)** Percentage of  
154 infected spleen monocytes expressing Fas at their surface (left), and the mean fluorescence  
155 intensity (MFI) of Fas signal (right), 3 days after iv inoculation of KIE16P mice with  $10^4$  CFU of  
156 CC4-WT or CC4 $\Delta$ inlB. **(l)** Proportion of dye-positive infected monocytes in the blood and the  
157 spleen after iv infection of KIE16P mice with  $10^4$  CFU of CC4-WT or CC4- $\Delta$ inlB. The repartition  
158 of the estimated half-lives and the median are shown besides each graph. Data were obtained from  
159 three independent experiments and are presented as mean  $\pm$  SD (a, b, f, h-l) or median  $\pm$   
160 interquartile (box) and extreme values (lines) (d). Samples are compared with an unpaired student  
161 *t*-test (a, b, f, h-k), CFU in competition assays are compared with the Wilcoxon matched-pairs  
162 signed rank test (d), samples are compared with the Kruskal-Wallis test (d) and distribution of  
163 estimated half-lives (i) are compared with a Mood test. ns:  $p>0.05$ , \*:  $p<0.05$ , \*\*:  $p<0.001$ , \*\*\*:  
164  $p<0.0001$ .

165

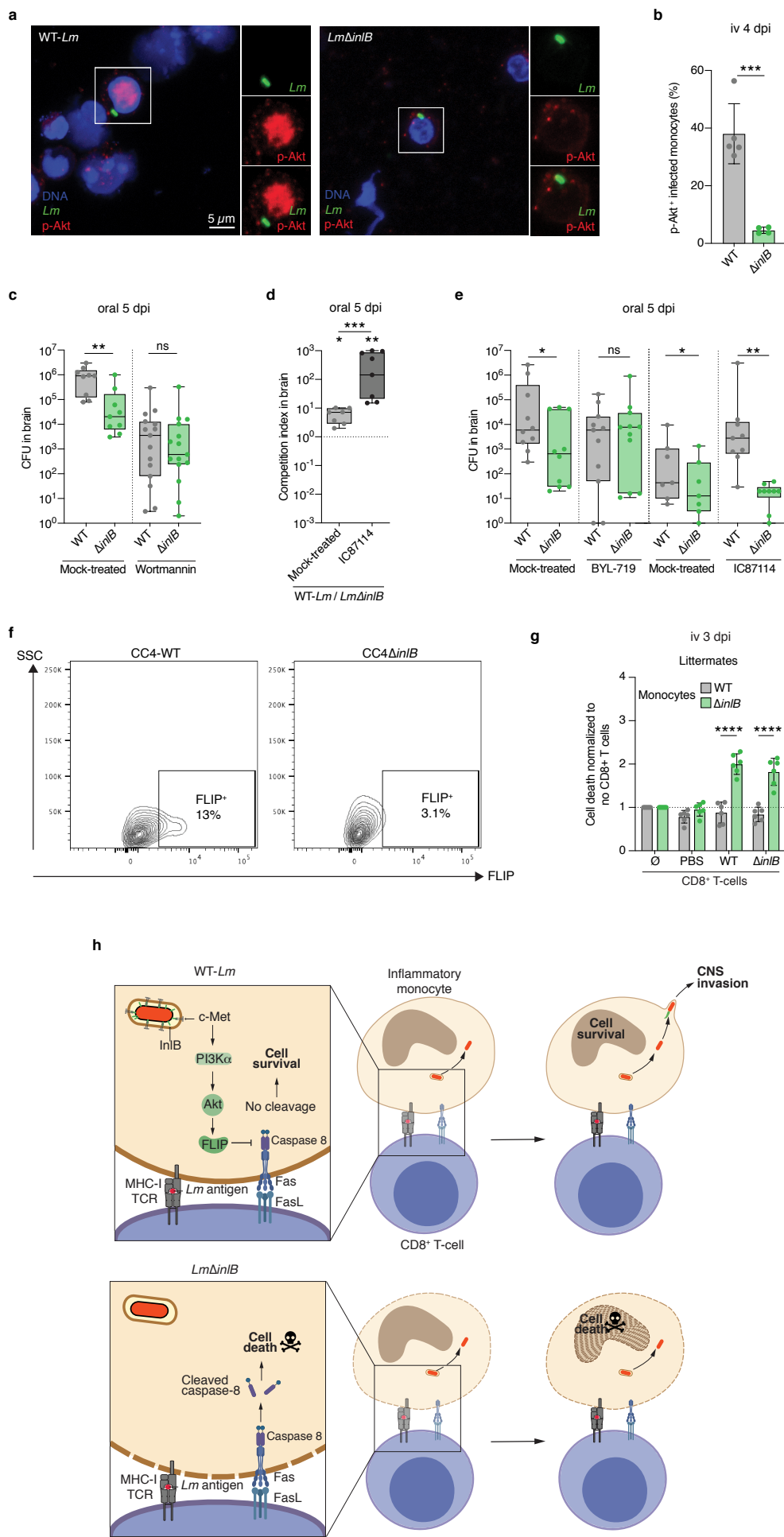
## Extended Data Figure 9



166 **Extended Data Figure 9. InlB recruits c-Met in infected monocytes. (a-c)** Representative  
167 fluorescence microscopy images of spleen monocytes harvested from KIE16P mice iv infected for  
168 4 days with  $10^4$  CFU of CC4-WT or CC4 $\Delta$ inlB, showing intra-vacuolar *Lm* surrounded with  
169 LAMP-1 (a), co-localizing with c-Met (b) and co-localizing with both c-Met and LAMP-1 (c). (a  
170 and b) are maximum intensity projection over a *z*-stack. (c) is a confocal single plane image. (d)  
171 Quantification of intracellular *Lm* co-localizing or not with c-Met and LAMP-1 in infected spleen  
172 monocytes harvested from KIE16P mice iv infected for 4 days with  $10^4$  CFU of CC4-WT or  
173 CC4 $\Delta$ inlB. Individual cells are plotted in top panel and samples are compared in bottom panel. (e)  
174 Percentage of *Lm* co-localizing with c-Met *in vitro* in Vero cells 15 min (left), 30 min (middle)  
175 and 45 min (right) after infection at MOI 50 with CC4 $\Delta$ inlB expressing either WT InlB, released  
176 InlB or cell wall-anchored InlB. (f) Bacterial load in the brain 5 days after oral inoculation with  
177  $2 \times 10^8$  CFU of 1:1 of CC4-WT and CC4 $\Delta$ inlB, in KIE16P mice treated with capmatinib, related to  
178 Fig. 4a. Data were obtained from three independent experiments (e-f) or from three microscopic  
179 field of views (d). Median number of bacteria in each intracellular compartment were compared  
180 with the Mann-Whitney test (d), proportions of c-Met associated bacteria (e) with Fischer's exact  
181 test, and CFU in competition assays (f) compared with the Wilcoxon matched-pairs signed rank  
182 test. ns:  $p > 0.05$ , \*:  $p < 0.05$ , \*\*:  $p < 0.01$ , \*\*\*\*:  $p < 0.0001$ .

183

# Extended Data Figure 10



184 **Extended Data Figure 10. InlB-mediated neuroinvasion involves the c-Met/PI3K $\alpha$ /FLIP**  
185 **pathway in infected monocytes.** (a) Representative fluorescence microscopy images of spleen  
186 monocytes harvested from KIE16P mice iv infected for 4 days with  $10^4$  CFU of CC4-WT or  
187 CC4 $\Delta$ inlB, showing phosphorylation of Akt. Images are maximum intensity projection over a z-  
188 stack. (b) Proportion of infected spleen monocytes positive for p-Akt signal 4 days after iv  
189 inoculation of KIE16P mice with  $10^4$  CFU of CC4-WT or CC4 $\Delta$ inlB. (c) Bacterial load in brain 5  
190 days after oral inoculation with  $2 \times 10^8$  CFU of 1:1 of CC4-WT and CC4 $\Delta$ inlB, in KIE16P mice  
191 treated with wortmannin, related to Fig. 4d. (d) Competition index in brain 5 days after oral  
192 inoculation with  $2 \times 10^8$  CFU of 1:1 of CC4-WT and CC4 $\Delta$ inlB, in KIE16P mice treated with PI3K $\delta$   
193 inhibitor (IC87114). (e) Bacterial load in the brain 5 days after oral inoculation with  $2 \times 10^8$  CFU  
194 of 1:1 of CC4-WT and CC4 $\Delta$ inlB, in mice treated with BYL-719 or IC87114, related to Fig. 4e  
195 and Extended Data Fig. 10d. (f) Representative dot plot of FLIP expression in infected  
196 inflammatory spleen monocytes, 3 days after iv inoculation with  $10^4$  CFU of CC4-WT or  
197 CC4 $\Delta$ inlB, related to Fig. 4f, g. (g) Level of caspase-3 cleavage of infected spleen monocytes,  
198 harvested 3 days after iv infection with  $10^4$  CFU of CC4-WT or CC4 $\Delta$ inlB of tamoxifen-treated  
199 *Rosa26-CreER*<sup>T2</sup> x *Cflar*<sup>+/+</sup> (FLIP<sup>+/+</sup>) littermate mice and incubated with CD8<sup>+</sup> T-cells from  
200 similarly infected mice at an effector to target ratio of 5, related to Fig. 4h. (h) Representation of  
201 InlB-activated pathway of infected monocytes survival to Fas-mediated cell death. Data were  
202 obtained from three independent experiments and are presented as median  $\pm$  interquartile (box)  
203 and extreme values (lines) (c-e) or mean  $\pm$  SD (b, g). CFU in competition assays are compared  
204 with the Wilcoxon matched-pairs signed rank test (c-e) and samples with a Mann-Whitney test (c-  
205 e) or an unpaired student *t*-test (b, g). ns:  $p > 0.05$ , \*:  $p < 0.05$ , \*\*:  $p < 0.01$ , \*\*\*:  $p < 0.001$ , \*\*\*\*:  
206  $p < 0.0001$ .

**Movie S1. Polymerization of actin comet tail by *Lm* within a monocyte adhering to the blood-brain barrier.**

CX3CR1<sup>GFP/+</sup> E16P KI humanized mice were infected with  $5 \times 10^5$  CFUs of CC6 (isolate 2009-01092) via iv route. Mice were sacrificed 48 hours post infection. CX3CR1<sup>+</sup> are labeled in green, *L. monocytogenes* in red, actin (phalloidin) in white and nuclei (Hoechst) in blue. Forty-six optical sections of a 20  $\mu$ m thick brain sample were imaged with a Zeiss LSM700 confocal microscope. 3D reconstruction was performed using the Arivis Vison 4D software.